

Giant Coupling Effects in Confined ^4He Near T_λ

J.K. Perron · F.M. Gasparini

Received: 21 June 2010 / Accepted: 22 November 2010 / Published online: 10 December 2010
© Springer Science+Business Media, LLC 2010

Abstract Superfluid ^4He shares with superconductors a transition into a low temperature state where the order parameter is a wave function. For the low temperature superconductors, which have a large zero temperature correlation length, this results in well known Josephson effects reflecting the overlap of the wave function across barriers and weak links. Similar phenomena are harder to realize for ^4He because the zero temperature correlation length is of the order of interatomic dimensions. The fact that for ^4He the critical region, where the correlation length diverges, is accessible experimentally leads to a possible new kind of coupling. This differs from that of a superconductor in the sense that critical fluctuations are important. We have seen such coupling whereby two regions of confined ^4He interact and influence their respective thermodynamic behavior (Perron et al. in Nat. Phys. 6:499–502, 2010). This interaction extends over length scales which are much larger than the correlation length. We describe measurements of heat capacity and superfluid density which illustrate this behavior.

Keywords Helium four · Superfluid transition · Weak links effects · Finite size effects · Critical phenomena · Finite size scaling · Coupling effect · Correlation lengths effects

1 Introduction

Over the years there have been many experiments on the superfluid transition of ^4He confined in packed powders and porous media, as well as better controlled geometries

J.K. Perron · F.M. Gasparini (✉)
Department of Physics, The University at Buffalo, State University of New York, Buffalo,
NY 14260, USA
e-mail: fmg@buffalo.edu

[2–4]. In many of these cases the interpretation of data is not clear because the geometry of confinement is not well characterized, and, just as importantly, the collective behavior or coupling across different spacial confinements is not well understood. Specifically, and most simply, consider a confinement in two well characterized and adjoining small regions. One may think of these regions as representing two separate thermodynamic phases which order at distinct temperatures. In each region this temperature is dictated by the smallest confinement size and the geometry of confinement i.e. for a given small dimension L the thermodynamic response will differ if L represents the thickness of a film or the radius of a cylindrical pore or a spherical cavity. If one considers two adjoining confinements at small dimension L and L' , then the joint behavior raises questions of the interactions or mutual influence between these two phases. From the point of view of critical phenomena, one may think of this interaction extending to a distance of the order of the correlation length, $\xi = \xi_0 |T/T_\lambda - 1|^{-\nu} \equiv \xi_0 t^{-\nu}$. With $\nu \simeq 2/3$ and ξ_0 of the order of interatomic dimensions, one can see that this would suggest coupling on a scale of micrometers for $t = 10^{-6}$.

Another way of looking at the coupling is to consider the specific order parameter for ^4He . This is a wave function, hence coupling may be described in the same way as for superconductors leading to the concept of wave function overlap or matching at the interface between two phases. This would lead to the familiar Josephson effects [5]. These have indeed been observed [6, 7] with weak links of small dimensions whereby at some point near T_λ one has $L \sim \xi$. A question arises in this context as to what constitutes a ‘weak link’ for ^4He . For the low temperature superconductors, which have a large value of ξ_0 and fluctuations are relegated to an experimentally inaccessible region, the answer is that a weak link is one of small dimension $L \sim \xi_0$. For ^4He , where fluctuations dominate the critical region on both sides of the transition, the answer as to what constitutes a weak link is not clear. Recent experiments, which were designed to look at correlation-length scaling of confined helium, have shown that coupling between regions of different confinement extends to distances much larger than ξ both above and below T_λ^1 . Indeed, there have been tunneling experiments with high T_c superconductors, where ξ_0 is also small and fluctuations are important, where tunneling was observed over length scales much larger than expected [8, 9].

In this paper we first discuss our measurement techniques, then present our results followed by some concluding remarks.

2 Experiment

Our experiments utilize the technique of direct wafer bonding of patterned silicon wafers to achieve a well-defined confinement for ^4He [10]. The construction of these cells involves oxide growth, lithography to define a pattern, a weak room temperature initial bonding, and a final high temperature annealing which produces a strong irreversible bond. These techniques have been described in greater detail in previous publications [10, 11]. The confinement geometry relevant to the present work is sketched in Fig. 1. In this schematic rendering we show a cross section of helium

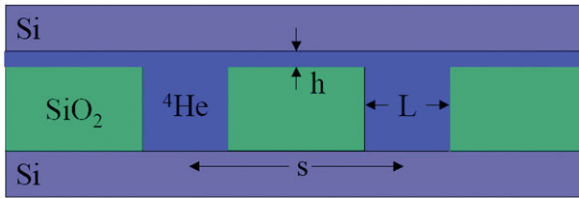


Fig. 1 (Color online) Schematic arrangement of boxes of volume L^3 and connecting channels or film linking them. L is either 1 or 2 μm . The height h is in the range of 10–30 nm. Cells constructed this way, from 5 cm silicon wafers, have 10^7 – 10^8 boxes and contain a few micromoles of helium

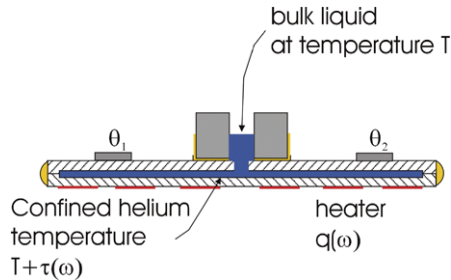


Fig. 2 (Color online) Schematic arrangement of the silicon cell. There are two germanium thermometers epoxied to the top wafer, θ_1, θ_2 . A resistive film in the shape of a spiral is evaporated on the bottom, the red lines. A cylindrical piece of silicon is epoxied to the top wafer. About 1 mm^3 of liquid in the center region gives a marker for the bulk transition T_λ

confined in boxes of volume L^3 linked by either a channel or a uniform film of thickness h . A cell will have approximately 10^7 to 10^8 boxes formed on a 5 cm diameter wafer.

For a system as depicted in Fig. 1 the superfluid transition will take place in two steps. The boxes will be the first to undergo a transition at a higher temperature than the film. At this point the order parameter in each box will have random phases because the connecting film will remain normal. When the film becomes superfluid at a lower temperature, global phase coherence will be established. It remains to be determined experimentally, for a given geometry, if there is sufficient coupling of the boxes through the connecting film to lead to a collective effect. Also part of this collective effect is how much the superfluid boxes will influence the normal film via a proximity effect.

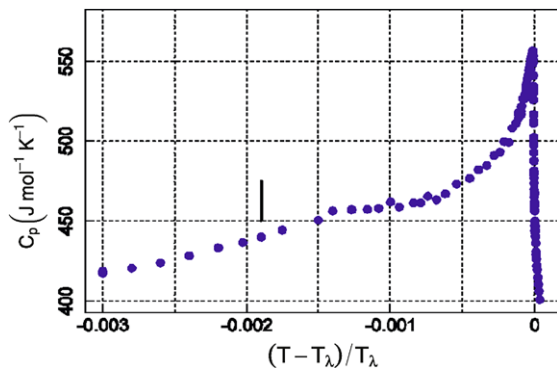
The arrangement of the cell to measure heat capacity is shown schematically in Fig. 2. There are two germanium thermometers epoxied to the cell θ_1, θ_2 . A spiral heater is evaporated on the bottom. What is not shown are weak thermal contacts to two temperature-regulated stages, one is kept colder than the cell the other warmer. The cell is given a temperature oscillation with the heater at a frequency ω . The temperature oscillation $\tau(\omega)$ is picked up with one of the thermometers. The other thermometer is used to regulate the average temperature T of the cell. From the amplitude of the oscillations one can obtain the heat capacity. The equations describing this behavior are given in Ref. [11]. To measure the superfluid fraction, the same technique is used, except that, in the presence of the superfluid, heating can result in

a Helmholtz resonance whereby the superfluid moves into the cell and is driven out by the resulting change in the chemical potential. The equations for this Adiabatic Fountain Resonance (AFR) have been derived [12]. The superfluid fraction ρ_s/ρ is proportional to the square of the resonant frequency ω_0^2 . Some typical numbers for these measurements are as follows. The temperature oscillations are of the order of a few μK . These can be resolved to ~ 40 nK by signal averaging for several minutes at each fixed temperature. Samples of ^4He are in the range 1–40 μmol . The heat capacity of the empty cell is in the range 20–100 $\mu\text{J/K}$ near T_λ . In the AFR measurement, we find quality factors as high as 10^3 far from the superfluid transition. Values for ω_0 can be obtained either from the temperature oscillations or from the phase difference between the drive signal and the signal picked up by the thermometer. Mass movement in and out of the cell at resonance is in the range of 10^{-11} – 10^{-12} mol.

3 Experimental Results and Discussion

The observation of coupling and proximity effects resulted from an attempt to verify finite size scaling for zero-dimensional crossover. For this, we obtained data for two cells, one with boxes of $(1 \mu\text{m})^3$ filled via channels $19 \text{ nm} \times 1 \mu\text{m} \times 1 \mu\text{m}$; and another, with boxes of $(2 \mu\text{m})^3$ filled via channels $10 \text{ nm} \times 2 \mu\text{m} \times 2 \mu\text{m}$, where the first number is the height and the other two are the length and width [13, 14]. The surprising result from these data was that there was no scaling throughout the critical region [15]. Further, the specific heat for the smaller boxes appeared too large relative to the bigger boxes. In neither of these two cases was the amount of helium in the channels such as to give a significant contribution to the overall heat capacity [15]. Also, in both cases, *the helium in the channels remained normal throughout the critical region of the helium in the boxes*. The overall lack of scaling was contrary to the behavior of confined helium where, especially in the case of 2D crossover, excellent scaling is obtained above T_λ , and over a *limited region* below T_λ [4]. To resolve this issue, we made a different cell of $(2 \mu\text{m})^3$ boxes. We spaced the boxes at $S = 6 \mu\text{m}$ center to center and, instead of filling channels, we left an open film of height $31.7 \pm 0.1 \text{ nm}$. The heat capacity of helium obtained with this cell is shown in Fig. 3 over a limited range of temperatures. From Fig. 3 one can see that the heat capacity has a large signal associated with the boxes near $t \approx 0$, and a small signal coming from the film at a

Fig. 3 (Color online) Heat capacity of an array of $(2 \mu\text{m})^3$ boxes connected with a film of 31.7 nm. The large peak reflects the helium in the boxes. The small bump at $t \approx 0.0014$ reflects the contribution of the film. The marker at $t = (1.9 \pm 0.07) \times 10^{-3}$ is the position of the expected maximum for a uniform 31.7 nm film



reduced temperature of $(-1.4 \pm 0.07) \times 10^{-3}$. The interesting point about the film's signal is that the maximum should occur at the position indicated by the vertical line. This is known from measurements of other planar films not influenced by the presence of helium in another geometry [4]. *Thus the first evidence of a proximity effect is the shift of the maximum of the film to a warmer temperature.* Next, one can ask if the magnitude of the film's specific heat is enhanced. To answer this, one can calculate the contribution of a uniform film of 31.7 nm by using empirical scaling functions for planar data [4]. This can be done to temperatures close to the specific heat maximum but not to lower temperatures. By subtracting this calculated contribution one obtains the specific heat of the helium in the boxes [1]. One can compare this with the earlier data of $(2 \mu\text{m})^3$ boxes linked with a channel. This is shown on a semilog plot in Fig. 4 [1]. One can see that over most of the temperature region these data overlap. In the region where the film orders however, the subtraction of the heat capacity of a uniform film has left an excess signal which is shown more clearly in the inset. *This excess signal is due to the enhancement of the heat capacity of the film due to the presence of the boxes.* This is the second evidence of a proximity effect. The other set of data, by design, have negligible contribution from the helium in the connecting channels, and show no structure. Another indication of the influence of the boxes on the behavior of the film can be seen in the superfluid density. The superfluid flow in the film is over a 'bed' of already superfluid boxes. The resulting superfluid fraction obtained from the AFR measurements is shown in Fig. 5. One can see from this figure that the superfluid fraction persists to a higher temperature than expected [4] (the vertical line) and to a lower value than the expected Kosterlitz-Thouless (KT) jump [16, 17] for a uniform 31.7 nm film (the crossing horizontal dashed line). This lower value in the KT jump is significant if one considers that in an AFR measurement one cannot obtain ρ_s/ρ too close to the transition because one loses the resonance due to dissipation. An example of this can be seen in Fig. 5 for a uniform 48.3 nm film which was measured to a value close to, but slightly larger than the expected KT jump—the dashed line just below the last point for these data. Of course, all the values of ρ_s/ρ for the 31.7 nm film are enhanced throughout the critical region. This enhancement however, cannot be quantified at present since the corresponding behavior for a uniform film of this thickness has not been measured and, contrary to the specific heat, cannot be calculated from existing data. To appreciate how significant the influence of the superfluid boxes is on the film, we note that at the temperature where the film orders the liquid in the boxes may be viewed as bulk-like. The bulk correlation length at this temperature is 24 nm. The separation between boxes is 4000 nm edge to edge. *Thus, the influence of the boxes extends over distances significantly longer than the correlation length.* The behavior of the superfluid density is further evidence for a proximity effect on the film.

We examine now the problem which triggered the present study: the lack of correlation-length scaling in the original $(2 \mu\text{m})^3$ and $(1 \mu\text{m})^3$ specific heat data [15]. One finds, as shown in Fig. 4, that the specific heat of the present boxes (away from where the film orders) matches well with the original $(2 \mu\text{m})^3$ boxes which were coupled through a shallow channel 10 nm high over an edge-to-edge distance of 2 μm . Since these two independent sets of data agree, it would seem then that the fault for the lack of scaling is in the $(1 \mu\text{m})^3$ boxes. These boxes were patterned closer together, at a distance of 1 μm edge to edge, and the channel was nearly twice as high

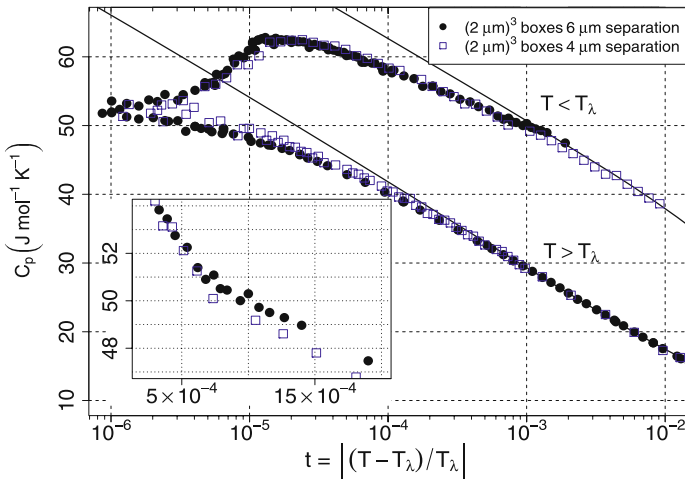
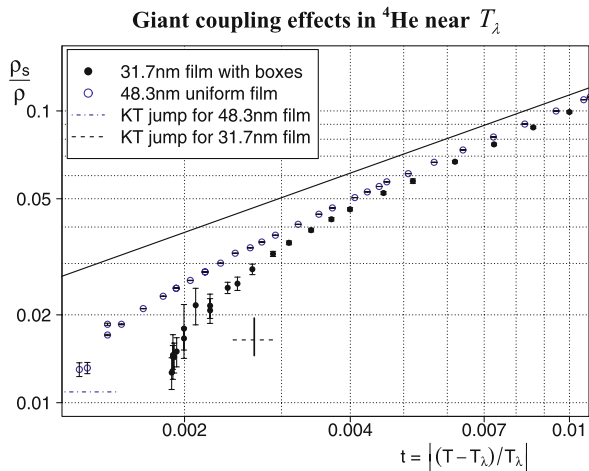


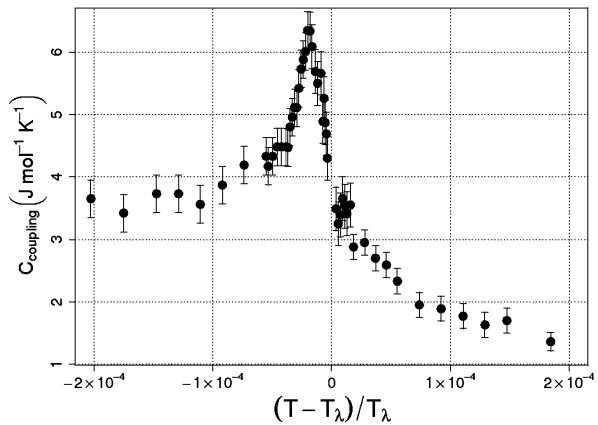
Fig. 4 (Color online) Specific heat near the superfluid transition for two samples of helium confined in $(2 \mu\text{m})^3$ boxes at different separations and connected either through a film or a channel [1]. The inset shows the region where the connecting film of 31.7 nm becomes superfluid

Fig. 5 (Color online) Superfluid fraction for two films of helium: One, at 31.7 nm, is in the presence of already superfluid boxes [1]; the other is a uniform film. The film in the presence of the boxes has a larger superfluid density than expected and its transition temperature is shifted to higher temperatures



at 19 nm. Given this, it is reasonable to assume that this lack of scaling is due to a collective or coupled behavior in these data. Clearly, in the limit that these boxes are placed even closer together, one would expect that an even stronger coupling would lead to 2D behavior. This would imply a yet larger specific heat [18]. To see the extent of this coupling one can assume that scaling holds and examine the excess signal in the $(1 \mu\text{m})^3$ boxes. The result of this analysis is shown in Fig. 6 [1]. These data show that C_{coupling} is quite substantial with a marked peak very close to where the original data have a maximum. The peak amounts to $\sim 10\%$ of the total signal as shown below. One also notes, for instance, that the bulk correlation length at $t = 10^{-4}$ is 0.07 and 0.17 μm on the warm and cold side respectively. The separation of the boxes

Fig. 6 Excess specific heat due to coupling through a 19 nm channel 1 μm wide in an array of $(1\ \mu\text{m})^3$ boxes spaced 1 μm edge to edge [1]



is ~ 5 – 10 times larger at this temperature. Thus in this instance, as well as with the behavior of the 31.7 nm film, the coupling extends to distances much larger than the correlation length. In the case of the specific heat the coupling clearly extends to the normal side. Thus the effect displayed in these data goes beyond Josephson coupling and must be connected with the role that fluctuations play at the superfluid transition.

4 Remarks

There are some similarities to our ‘two step’ transition as displayed in Fig. 3 to the calculation by Ferdinand and Fisher [19] for a modified two-dimensional Ising model which one might describe as ‘layered’. Here one considers n rows of sites with coupling of strength J and then one row of weaker coupling J' . The resultant specific heat can be calculated exactly and shows a broad maximum corresponding to ordering within the strip (the specific heat is broad because the strip is of finite width) and then a much sharper peak at lower temperature, reflecting the lower value of J' . It is at this lower temperature that long range order onsets throughout the lattice. Helium is of course not an Ising system so it differs in details. In particular, there is no sharp transition when global ordering takes place with the boxes-film system. Even if the coupling were very strong, the best one could expect is 2D crossover. This would produce a rounded specific heat albeit larger than that for the present data. Thus, the 2D crossover as function of the separation of the boxes, would be an interesting future experiment.

We also note that a two-step transition was also observed in specific heat of helium condensed in 0.2 nm diameter Nuclepore filters [20]. This was explained as two transitions taking place in the capillary condensed phase filling a portion of the pores and in the film of 5.5 nm which is expected to be in equilibrium with this phase. What was not appreciated at the time was that, while the attribution of the two maxima was indeed correct, the movement of the low temperature (the film’s) heat capacity maximum to lower temperatures, as the capillary condensed phase was depleted, was too rapid to be explained by a convolution of two signals. It is very likely, in light of the present measurements, that the relatively larger capillary phase enhanced the

transition in the film just as we have seen in the much better controlled geometry of the boxes-film system. It would be difficult to extract quantitative results from these earlier data since it has been recognized that Nuclepore filters do not provide ideal cylindrical holes with smooth surfaces [21]. The surfaces are rough [22], and there are internal linkages amongst the holes [23], and, of course, connections along the surfaces of the filters via the film. All of this renders confinement in this medium rather unique. This has been discussed in Ref. [4]. Nevertheless the ‘two peak’ observation, and the magnitude and movement of the film’s heat capacity is very likely due to the same type of coupling as with the film-boxes system.

Another point of comparison with our results is the recently reported giant proximity effect in high T_c superconductors [8, 9]. In this work tunneling was studied between two superconducting samples of Lanthanum Strontium Copper Oxide (LSCO). Separating these superconductors was a layer of underdoped Lanthanum Copper Oxide (LCO). The correlation length in these superconductors is much like helium of the order of interatomic spacing, and order parameter fluctuations are important. What is found in this experiment is that tunneling could be observed through the LCO with thickness in the range of 1 to 20 nm in a temperature region where the LCO *by itself* would be normal. This is reminiscent of our own observation of superflow in a temperature region where the film *by itself* would be normal were it not for the presence of the helium in the boxes. A possible explanation for this large proximity effect in the LSCO-LCO-LSCO system has been suggested [24]. This involves phase fluctuations in the order parameter of the normal LCO. Thus, the giant coupling would not occur if the LCO were replaced by an ordinary metal. These authors refer to this behavior as a qualitatively different type of Josephson tunneling.

The influence of one confined phase on another can be calculated in mean field theory. Mamaladze and Cheishvili [25] considered the problem of calculating the superfluid fraction in a slit which connects into bulk helium. They did this using the Ginzburg Pitaevskii equation. One can modify this equation, as was done later by Mamaladze [26], to include a $2/3$ power-law dependence for the superfluid density and a logarithmic singularity for the specific heat. This theory yields a differential equation for the amplitude of the wave function. This can be matched at positions where there is an interface with either a wall or a different confinement. We have taken the Mamaladze and Cheishvili analytical solution with the modified temperature dependence of the coefficients and calculated the superfluid fraction as one enters a slit of 31.7 nm from bulk liquid. This would emulate the box-to-film interface. The result is shown in Fig. 7. Here x is the distance from the partition in angstroms, negative for the bulk liquid and positive for the slit. The slit is wide and has no boundaries in the y direction. The behavior of ρ_s/ρ is qualitatively as one would expect. Within the slit the superfluid fraction is raised as one approaches the bulk interface. This is most evident at the smallest values of the reduced temperature when the correlation length is the largest. The bulk is affected negatively close to the slit, $x = 0$, where the superfluid fraction is reduced. At $t = 0.0025$, which is the smallest value at which the superfluid fraction is calculated, the correlation length in this theory is 87 angstroms. Thus there are significant effects in this theory within 2–3 correlation lengths. This is the distance one might expect on the basis of Josephson-like coupling of the two phases. The observations in our experiments show effects over much larger scales.

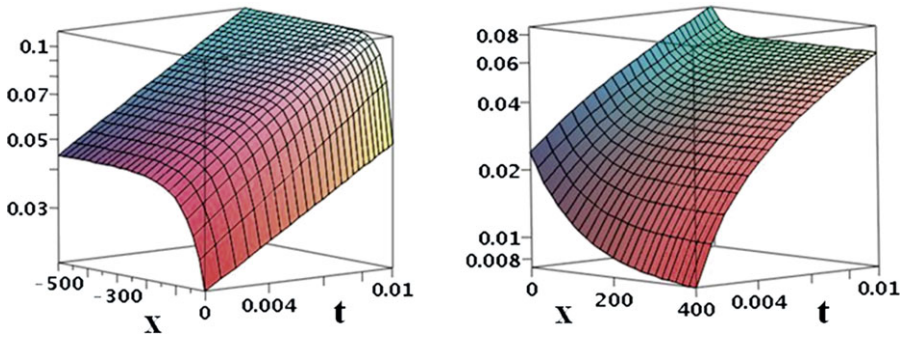
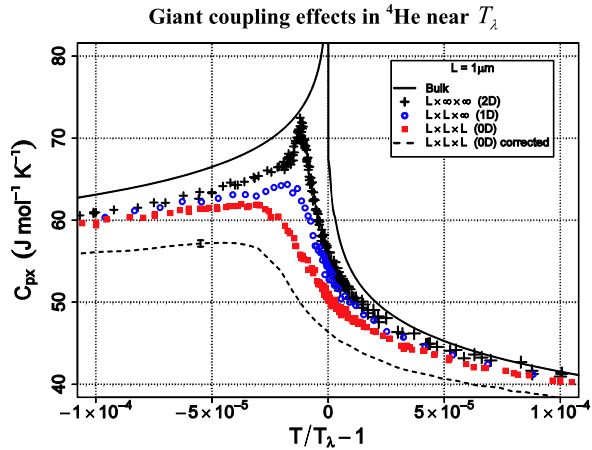


Fig. 7 (Color online) The local superfluid density as function of position x , in angstroms, and reduced temperature t as one moves away from the slit onto the bulk liquid (negative x), and into the slit (positive x)

Fig. 8 (Color online) Role of dimensionality on the confined specific heat [18]. The dashed curve represents the 0D data after the correction from coupling



In previous measurements Kimball et al. reported data at 1 μm confinement for a film, channel and box geometry corresponding to 2D, 1D, and 0D crossover [18]. These data, plotted in Fig. 8, showed for the first time the role that dimensionality plays on the specific heat via the quenching of critical fluctuations in progressively more directions. One can see from this figure that, as dimensionality is reduced, the specific heat is successively lowered, and its maximum shifted to lower temperatures. In light of the coupling identified with the 1 μm box confinement, one may correct the data for 0D crossover to reflect the enhancement shown in Fig. 6. The dashed curve reflects this correction. One can see that the correction, as mentioned earlier, is quite substantial. One may conclude that quenching fluctuations in all three dimensions affects the specific heat to a much greater extent than previously expected.

Note added in proof We have now measured the superfluid density of a uniform film of 33.6 nm thickness. We find that the comments regarding Fig. 5 about the shift in T_c and the enhancement in ρ_s/ρ are fully justified. In particular, we find that the enhancement of ρ_s/ρ for the film-boxes system relative to a uniform film extends

to temperatures where the bulk correlation length is $\sim 1/600$ of the separation of the boxes.

Acknowledgements This work is supported by the US National Science Foundation, grant No. DMR-0605716; the Cornell Nanoscale Science and Technology Facility, project No 526-94; and, funding from the University at Buffalo.

References

1. J.K. Perron, M.O.K. Kimball, K.P. Mooney, F.M. Gasparini, *Nat. Phys.* **6**, 499–502 (2010)
2. J.D. Reppy, *J. Low Temp. Phys.* **87**, 205–245 (1992)
3. F.M. Gasparini, I. Rhee, in *Progress in Low Temperature Physics*, vol. 13, ed. by D.F. Brewer (North Holland, Amsterdam, 1992), pp. 1–90
4. F.M. Gasparini, M.O.K. Kimball, K.P. Mooney, M. Diaz-Avila, *Rev. Mod. Phys.* **80**, 1009–1059 (2009)
5. M. Tinkham, *Introduction to Superconductivity* (McGraw-Hill, New York, 1996)
6. K. Sukhatme, Y. Mucharsky, T. Chui, D. Pearson, *Nature* **411**, 280–283 (2001)
7. E. Hoskinson, Y. Sato, R.E. Packard, *Phys. Rev. B, Condens. Matter Mater. Phys.* **74**, 100509 (2006)
8. I. Bozovic, G. Logvenov, M.A.J. Verhoeven, P. Caputo, E. Goldobin, M.R. Beasley, *Phys. Rev. Lett.* **93**, 157002 (2004) and references therein
9. E. Polturak, G. Koren, D. Cohen, E. Aharoni, *Phys. Rev. Lett.* **67**, 3038–3041 (1991)
10. I. Rhee, D.J. Bishop, A. Petrou, F.M. Gasparini, *Rev. Sci. Instrum.* **61**, 1528–1536 (1990)
11. S. Mehta, M.O. Kimball, F.M. Gasparini, *J. Low Temp. Phys.* **114**, 467–521 (1999)
12. F.M. Gasparini, M.O. Kimball, S. Mehta, *J. Low Temp. Phys.* **125**, 215–238 (2001)
13. M.O. Kimball, Ph.D. Thesis, University at Buffalo, The State University of New York (2005)
14. K.P. Mooney, Ph.D. Thesis, University at Buffalo, The State University of New York (2006)
15. J.K. Perron, M.O.K. Kimball, K.P. Mooney, F.M. Gasparini, *J. Phys., Conf. Ser.* **150**, 032082 (2009)
16. M. Kosterlitz, D.J. Thouless, *J. Phys. C* **6**, 1181–1203 (1973)
17. D.R. Nelson, J.M. Kostelitz, *Phys. Rev. Lett.* **39**, 1201–1205 (1977)
18. M.O.K. Kimball, K.P. Mooney, F.M. Gasparini, *Phys. Rev. Lett.* **92**, 115301 (2004)
19. M.E. Fisher, *J. Phys. Soc. Jpn., Suppl.* **26**, 87–93 (1969)
20. T.P. Chen, M.J. Di Pirro, A.A. Gaeta, F.M. Gasparini, *J. Low Temp. Phys.* **26**(5/6), 927–944 (1977)
21. T.P. Chen, M.J. Di Pirro, B. Bhattacharyya, F.M. Gasparini, *Rev. Sci. Instrum.* **51**, 846–848 (1980)
22. S. Mhlanga, F.M. Gasparini, *Phys. Rev. B* **33**, 5066–5069 (1986)
23. D.T. Smith, K.M. Godshalk, R.B. Hallock, *Phys. Rev. B* **36**, 202–216 (1987)
24. D. Marchand, L. Covaci, M. Berciu, M. Franz, *Phys. Rev. Lett.* **10**, 097004 (2008)
25. Y.G. Mamaladze, O.D. Cheishvili, *Sov. Phys. JETP* **23**, 112 (1966); *Z. Eksp. Teor. Fiz.* **50**, 169 (1966)
26. Y.G. Mamaladze, *Ž. èksp. Teor. Fiz.* **52**, 729 (1967)